**Proceedings of the ASME 2009 International Design Engineering Technical Conferences & Computers and Information in Engineering Conference**
**IDETC/CIE 2009**
**August 30 - September 2, 2009, San Diego, California, USA**

**DETC2009-86959**

# SOME OBSERVATIONS ON HUMAN CONTROL OF A BICYCLE

**J.D.G. Kooijman**
**A.L. Schwab***
Laboratory for Engineering Mechanics
Faculty of 3mE
Delft University of Technology
Mekelweg 2, NL 2628CD Delft
The Netherlands
Email: jodikooijman@gmail.com
a.l.schwab@tudelft.nl

**Jason K. Moore**
Sports Biomechanics Laboratory
Department of Mechanical and Aeronautical Engineering
University of California,
One Shields Avenue
Davis, California 95616
Email: jkmoor@ucdavis.edu

## ABSTRACT

*The purpose of this study is to identify human control actions in normal bicycling. The task under study is the stabilization of the mostly unstable lateral motion of the bicycle-rider system. This is done by visual observation of the rider and measuring the vehicle motions. The observations show that very little upper-body lean occurs and that stabilization is done by steering control actions only. However, at very low forward speed a second control is introduced to the system: knee movement. Moreover, all control actions are performed at the pedaling frequency, whilst the amplitude of the steering motion increases rapidly with decreasing forward speed.*

## INTRODUCTION

Riding a bicycle is an acquired skill. At very low speed the bicycle is highly unstable. However, at moderate speed the bicycle is easy to stabilize. These observations are confirmed by a stability analysis on a simple dynamical model of an uncontrolled bicycle [1] and some experiments [2] and [3]. Although there is little established knowledge on how we stabilize a bicycle, two basic features are known: some uncontrolled bicycles can balance themselves given some initial speed, and one can balance a forward moving bicycle by turning the front wheel in the direction of the undesired lean. But when observing a rider on a bicycle, not only the handlebars are moving but also the upper body and other extremities. These rider body motions are even more profound when riding a motorcycle [4].

The purpose of this study is to identify the major human control actions in normal bicycling where we focus on the stabilizing task only, but not tracking. The identification is done by visual observation of the rider and measurement of the vehicle motions on an instrumented bicycle, see Fig. 1. In order to observe the human control actions a number of experiments were carried out. First a typical town ride was made to investigate what sort of actions take place during normal riding. After this, experiments were carried out in a controlled environment, on a large treadmill ($3 \times 5$ m), at various speeds. The same bicycle was used during all the experiments. The bicycle was ridden by two averagely skilled riders. Three riding cases were considered: normal bicycling, towing and normal bicycling with lateral perturbations. These experiments were carried out to identify the effect of upper body motion and the effect of the pedaling motion on the control. The rider was told to simply stabilize the bicycle and to generally ride in the longitudinal direction of the treadmill; no tracking task was set. Recorded data were the rigid body motions of the bicycle rear frame and the front assembly. The rider motion relative to the rear frame was recorded via video.

*Address all correspondence to this author.


Figure 1. THE INSTRUMENTED BICYCLE WITH CAMERA BOOM AND VIDEO CAMERA LENS (1). ON THE REAR RACK THE MEASUREMENT COMPUTER (2), VIDEO CAMCORDER (3) AND BATTERY PACKS (4) ARE POSITIONED. MEASURED SIGNALS ARE THE STEER ANGLE AND STEER-RATE (5), REAR FRAME LEAN- AND YAW-RATE (6) AND FORWARD SPEED (7).

## INSTRUMENTED BICYCLE

A standard Dutch bicycle, a 2008 model Batavus Browser was chosen for the experiments and is shown in Fig. 1. This is a bicycle of conventional design, fitted with a 3-speed SRAM rear hub and coaster brakes. Some of the peripheral components were removed in order to be able to install measurement equipment and sensors (see Tab. 1).

The bicycle was equipped with a 1/3" CCD color bullet-camera with 2.9mm (wide angle) lens. The camera was located at the front and directed towards the rider and rotated 90 degrees clockwise to get portrait aspect ratio. The video signal was recorded, via the AV-in port, on DV tape of a Sony Handycam located on the rear rack of the bicycle. The bullet camera was placed horizontally, approximately 65 cm in front of the handlebars and 1.2 m above the ground and held in place by a carbon-fiber boom connected to the down-tube of the rear frame, see Fig. 1.

A National Instruments' CompactRIO (type CRIO-9014) computer was used for data collection. The CompactRIO was installed on the rear rack of the bicycle. It was fitted with a 32-channel, 16 bit analogue input module and a 4-channel, 16 bit analogue output module as well as a CRIO WLAN-MH1000 wireless modem by S.E.A. Datentechnik GmbH for a wireless connection with a "ground station" router, to which a laptop was connected. The measurement system is able to run autonomously once a measurement sequence is initiated. The CompactRIO was powered by a 11.1V, 1500mAh Lithium Polymer battery which was also placed on the bicycle's rear rack.

Figure 2. SCREEN-SHOT OF VIDEO MADE WITH THE BULLET CAMERA CONNECTED TO THE BICYCLE FRAME, FACING REARWARDS, SHOWING THE RIDER POSITION DURING NORMAL CYCLING.

The recorded signals were the lean, yaw and steer rates, the steer angle, the rear wheel speed and the pedaling cadence frequency. The angular rates were measured using 3 Silicon Sensing CRS03, single axis angular rate sensors with a rate range of $\pm$ 100 deg/s. The steer angle was measured using a potentiometer placed on the rear-frame against the front of the head tube and connected via a belt and pulley pair. The angular rate sensors and the angular potentiometer were powered by a 4.8V, 2100mAh Nickel Cadmium battery. The forward speed was measured by measuring the output voltage of a Maxon motor that was driven by the rear wheel. The cadence frequency was measured by a reed-relay placed on the rear frame, and a magnet placed on the left crank-arm.

## TOWN RIDE EXPERIMENT

As a first step in human rider control observations a short, 15 minute, ride around town was carried out. This experiment took place under normal riding conditions (dry weather, daylight, etc.), on roads that the rider was familiar with. The course covered included a round-a-bout, dedicated cycling paths, speed-bumps, pavement, normal tarmac roads, tight bends in a residential area and the rider had to stop at a number of traffic lights. There were no special precautions taken and the experiment was carried out amongst other traffic. From the recorded video material and measured data two observations were made:

1. The video material showed that there was very little upper body lean relative to the rear-frame, carried out during the whole ride. The relative upper body lean that was noted appeared to be as a result of pedaling. Only in the last few seconds prior to a sharp corner was an upper body lean angle observed - indicating that the lean was carried out because of a sudden heading change.
2. The recorded data, part of which is shown in Fig. 3, clearly shows that only very small steering actions ($\pm$ 3 deg) are

Table 1. USED SENSORS

| Measurement | Sensor Type | Manufacturer | Type | Specification |
|---|---|---|---|---|
| Steer-rate<br>Yaw-rate<br>Lean-rate | MEMS Angular Rate | Silicon Sensing | CRS03 | Full range output $\pm$ 100 deg/s |
| Steer angle | Potentiometer | Sakae | FPC40A | 1 turn, conductive plastic, Servo mount |
| Forward speed | DC-motor | Maxon | 2326-940-12-216-200 | Graphite brush motor with a 5cm diameter disk on the shaft |
| Cadence | Reed relay and magnet | - | - | Kitchen magnet |

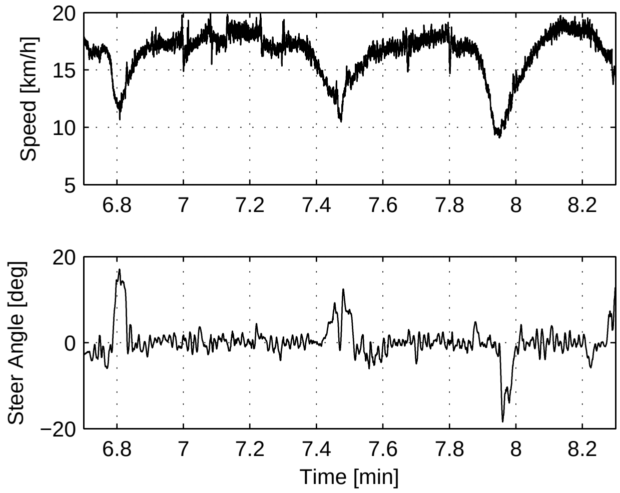


Figure 3. DATA COLLECTED DURING A RIDE AROUND TOWN. UPPER GRAPH SHOWS THE SPEED THE BICYCLE WAS TRAVELING AT, THE LOWER THE STEERING ANGLE.

carried out during most of the the experiment. Only when the forward speed has dropped, prior to making a corner, are large steer angles ($\pm$ 15 deg) seen.

## TREADMILL EXPERIMENTS

Riding a bicycle on the open road amongst normal traffic subjects the bicycle-rider system to many external disturbances such as side wind, traffic and road unevenness. To eliminate these disturbances a more controlled environment was selected to carry out further studies on human rider control for stabilizing tasks. The experiments were carried out on a large ($3 \times 5$ m) treadmill, shown in Fig. 4. The dynamics of a bicycle on a treadmill were shown to be the same as for on flat level ground by [3].

Table 2. RIDER CHARACTERISTICS

| Rider | Weight [kg] | Height [cm] | Age |
|---|---|---|---|
| 1 | 102 | 187 | 53 |
| 2 | 72 | 183 | 26 |

Figure 4. LARGE TREADMILL, 3X5 M, MAX SPEED 35 KM/H, COURTESY OF THE FACULTY OF HUMAN MOVEMENT SCIENCES, VU UNIVERSITY AMSTERDAM.

The experiments were carried out by two, male, average ability, riders of different age and build on the same bicycle. The saddle height was adjusted for each rider to ensure proper seating for bicycling. The rider characteristics are given in Tab. 2. For both riders very similar results were found. The data and figures given in this paper were collected with rider 1.

The uncontrolled dynamics of the bicycle rider combination can be described by the linearized model of the bicycle [1]. This model consists of four rigid bodies, viz. the rear frame with rigid rider connected, the front handlebar and fork assembly, and the two wheels. These are connected by ideal hinges and the wheels

Table 3. BICYCLE PARAMETER VALUES

| parameter | symbol | value for bicycle & rider |
|---|---|---|
| wheel base | $w$ | 1.12 m |
| trail | $c$ | 0.055 m |
| steer axis tilt ($\pi/2$ − head angle) | $\lambda$ | 0.375 rad |
| gravity | $g$ | 9.81 N kg$^{-1}$ |
| forward speed | $v$ | various m s$^{-1}$ |
| **R***ear wheel R* | | |
| radius | $r_{\mathrm{R}}$ | 0.342 m |
| mass | $m_{\mathrm{R}}$ | 3.12 kg |
| mass moments of inertia | $(I_{\mathrm{R}xx}, I_{\mathrm{R}yy})$ | (0.078, 0.156) kg m$^2$ |
| *rear* **B***ody and frame B* | | |
| position centre of mass | $(x_{\mathrm{B}}, z_{\mathrm{B}})$ | (0.30, −1.08) m |
| mass | $m_{\mathrm{B}}$ | 116 kg |
| mass moments of inertia | $\begin{bmatrix} I_{\mathrm{B}xx} & 0 & I_{\mathrm{B}xz} \\ 0 & I_{\mathrm{B}yy} & 0 \\ I_{\mathrm{B}xz} & 0 & I_{\mathrm{B}zz} \end{bmatrix}$ | $\begin{bmatrix} 16.784 & 0 & -3.616 \\ 0 & I_{\mathrm{B}yy} & 0 \\ -3.616 & 0 & 6.035 \end{bmatrix}$ kg m$^2$ |
| *front* **H***andlebar and fork assembly H* | | |
| position centre of mass | $(x_{\mathrm{H}}, z_{\mathrm{H}})$ | (0.88, −0.78) m |
| mass | $m_{\mathrm{H}}$ | 4.35 kg |
| mass moments of inertia | $\begin{bmatrix} I_{\mathrm{H}xx} & 0 & I_{\mathrm{H}xz} \\ 0 & I_{\mathrm{H}yy} & 0 \\ I_{\mathrm{H}xz} & 0 & I_{\mathrm{H}zz} \end{bmatrix}$ | $\begin{bmatrix} 0.345 & 0 & -0.044 \\ 0 & I_{\mathrm{H}yy} & 0 \\ -0.044 & 0 & 0.065 \end{bmatrix}$ kg m$^2$ |
| **F***ront wheel F* | | |
| radius | $r_{\mathrm{F}}$ | 0.342 m |
| mass | $m_{\mathrm{F}}$ | 2.02 kg |
| mass moments of inertia | $(I_{\mathrm{F}xx}, I_{\mathrm{F}yy})$ | (0.081, 0.162) kg m$^2$ |

have idealized pure-rolling contact with level ground (no tire models). Reference [5] describes the method used to determine the properties for the instrumented bicycle/rider system. For the instrumented bicycle and rider. The instrumented bicycle/rider system parameters are given in Tab. 3 and, the linearized stability is depicted in Fig. 5. At low speed the important motion is the unstable oscillatory weave motion. This weave motion becomes stable around 18 km/h, the so-called weave speed. At higher speeds the non-oscillatory capsize motion becomes unstable but since this instability is so mild it is very easy to control. Summarizing: the instrumented bicycle rider combination is in need of human stabilizing control below 18 km/h and is stable above this speed.

For safety reasons the riders were fitted with a harness that was connected to the ceiling via a long climbing rope. This ensured that should the rider fall over no contact with the moving part of the treadmill would be made. Also a retractable dog leash was connected between the front of the harness and the treadmill kill switch. This ensured that the treadmill would immediately come to a halt, should the bicycle go too far back, reducing the chance that the bicycle could go off the end of the treadmill.

Three types of riding experiments were carried out: normal bicycling, towing and bicycling with lateral perturbations. The normal bicycling experiment was carried out to investigate what type of control actions a rider carries out to stabilize a bicycle. The towing experiment was carried out to remove the dominant

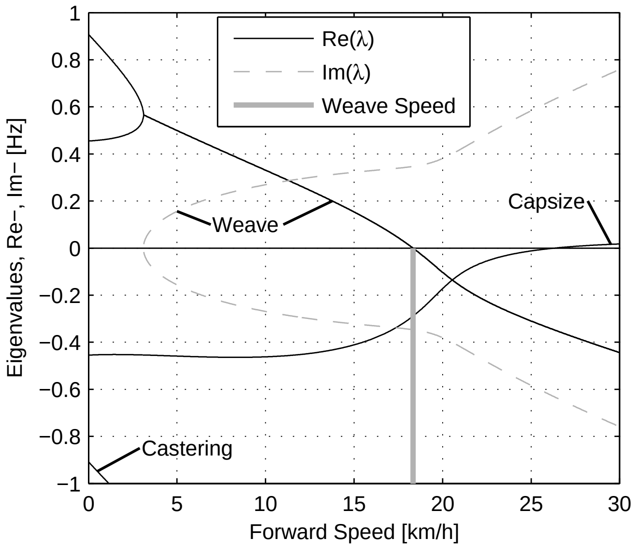


Figure 5. EIGENVALUES FOR THE LINEARIZED STABILITY ANALYSIS OF AN UNCONTROLLED BICYCLE-RIDER COMBINATION FOR THE STEADY UPRIGHT MOTION IN THE FORWARD SPEED RANGE OF 0-30 KM/H. SOLID LINES ARE REAL PARTS, DOTTED LINES ARE IMAGINARY PARTS. THE BICYCLE IS PRACTICALLY STABLE FROM THE WEAVE SPEED, 18 KM/H AND ABOVE.

pedaling motion, seen during the town-ride experiment, from the system. The bicycling with lateral perturbations was performed to investigate how the human rider recovers from an unstable situation which was simulated by applying a lateral impulse to the rear frame.

Each experiment was carried out at 6 different speeds: 30, 25, 20, 15, 10 and 5 km/h. In total 36 experiments were performed. During the normal bicycling and bicycling with lateral perturbations experiments the rider pedalled normally and used first gear during the 5 and 10 km/h runs. Second gear was used in the 15 and 20 km/h runs and third gear was used during the 25 and 30 km/h runs. The cadence varied between 24 rpm at 5 km/h and 80 rpm at 30 km/h. During the towing series of experiments the bicycle and rider were towed by a rope connected to the bicycle rear frame at the lower end of the head tube. The rider kept the pedals in the horizontal position during these experiments. The crank arm side that was placed forward was left to rider preference. During the lateral perturbations experiment the bicycle was perturbed by applying a lateral impulse to the rear frame. The impulse was applied by a manually actuated rope tied to the seat tube. The rider could not see the rope being actuated to ensure that the rider was unprepared, however, they knew the direction of the perturbation.

The riders were instructed to stay on the treadmill and to generally ride in the longitudinal direction of the treadmill but not to concentrate on their position on the treadmill in order to prevent the rider from performing a tracking task. Data was collected for 1 minute during each experiment with a 100Hz sample rate. Video footage can be found at the website [6].

### Normal Bicycling; Pedaling

Visual inspection of the video footage showed very little lean action during the experiment other than that resulting directly from the pedaling motion. During the low speed run at 5 km/h, the rider's upper body was almost stationary, i.e. it could be considered to be rigidly attached to the rear-frame. However at this speed the rider's knees showed significant lateral motion. This lateral knee motion can be seen in the video image in Fig. 6. A third observation was that the rider turned the handlebars more at lower speeds than at higher speeds.

Figure 6. SCREEN-SHOT OF NORMAL PEDALING AT LOW SPEED (5 KM/H) SHOWING LARGE LATERAL (LEFT) KNEE MOTION AND (RIGHT) STEERING ACTION. THE GREY VERTICAL LINE INDICATES THE MIDPLANE OF THE BICYCLE. NOTE THAT THERE IS ALMOST NO UPPER BODY LEAN PRESENT.

This third observation is confirmed by the measured steer angle data. Figures 7 and 8 show the time history of the steer angle for the experiments carried out at 20 and 5 km/h respectively. The standard deviation of the steer angle during the sixty seconds of measurement is also shown in the figures. At speeds above 20 km/h the average steer angle remains approximately constant. However the average magnitude of the steer angle grows by more than 500% when the speed is decreased from 20 km/h to 5 km/h. This increase in steer angle magnitude for the decreasing speeds is illustrated in Fig. 9.

The frequency content of the steering signal for the different forward speeds is shown in Fig. 10. The grey vertically dashed line indicates the rigid rider/bicycle weave frequency. Figure 10 clearly shows that at none of the speeds the rigid rider/bicycle weave frequency is a frequency in which the bicycle/rider system operates.

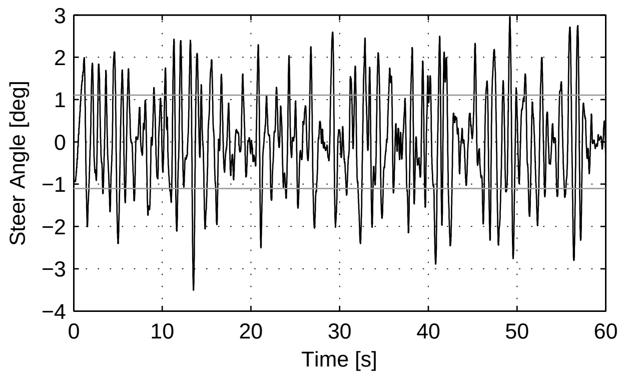


Figure 7. STEER ANGLE TIME HISTORY PLOT FOR 20 KM/H DURING NORMAL BICYCLING. THE STANDARD DEVIATION OF THE STEER ANGLE IS SHOWN IN GREY.

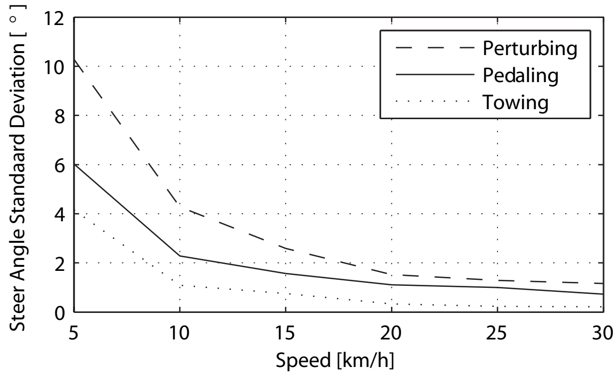


Figure 9. THE STANDARD DEVIATION OF THE STEER ANGLE FOR THE SIX DIFFERENT SPEEDS FOR THE THREE DIFFERENT EXPERIMENTS.

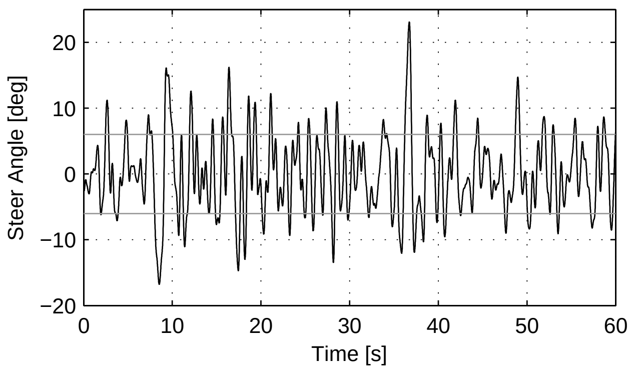


Figure 8. STEER ANGLE TIME HISTORY PLOT FOR 5 KM/H DURING NORMAL BICYCLING. THE STANDARD DEVIATION OF THE STEER ANGLE IS SHOWN IN GREY.

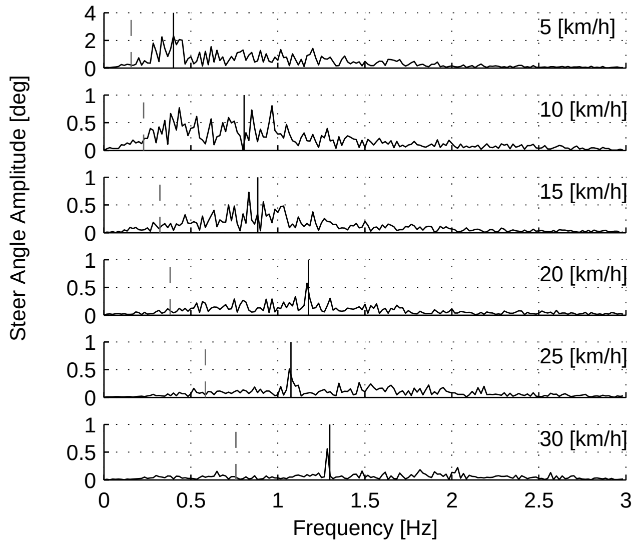


Figure 10. STEER ANGLE AMPLITUDE PLOT FOR THE SIX DIFFERENT SPEEDS FOR NORMAL PEDALING EXPERIMENT. SOLID VERTICAL LINE INDICATES THE PEDALING FREQUENCY. DASHED VERTICAL GREY LINE INDICATES THE BICYCLE & RIGID RIDER WEAVE EIGENFREQUENCY.

The black vertical dashed line in each of the plots in Fig. 10 indicates the measured pedaling frequency. The figure clearly shows that during normal pedaling most of steering action takes place at, or around, the pedaling frequency, irrespective of the speed that the bicycle is moving. The pedaling frequency is especially dominant in the steering signal at the highest speeds where practically all of the steering takes place in the pedaling frequency.

Figure 11 shows that if the steering signal is assumed to consist of just one frequency - namely the frequency with the largest amplitude, how this maximum amplitude reduces with increasing speed. This assumption becomes more valid with increasing speed as indicated by Fig. 10. The plot in Fig. 11 has a similar shape to the standard deviation plot in Fig. 9.

### Towing; No Pedaling

Visual inspection of the video footage revealed, similar to the normal bicycling experiment, that no upper body leaning at any of the measured speeds and that larger steer angles occurred at the slower speeds. However, unlike the normal bicycling experiment, no knee motion could be detected from the video footage at any of the speeds, other than small remnant motion as a result of slight steering deviations from straight ahead.

The recorded steer angle data also indicated that larger steer

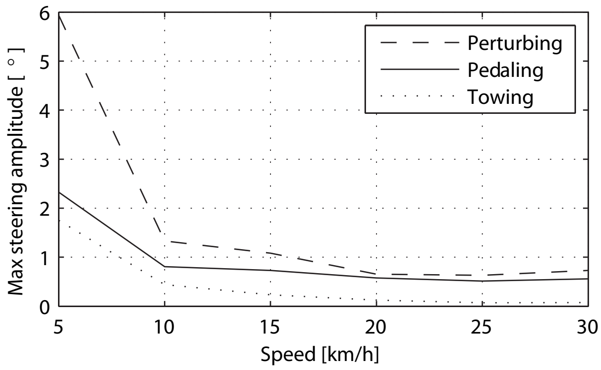


Figure 11. MAXIMUM STEERING AMPLITUDE IF THE STEERING SIGNAL CONSISTED OF A SINGLE FREQUENCY FOR THE THREE DIFFERENT EXPERIMENTS AT THE SIX DIFFERENT SPEEDS.

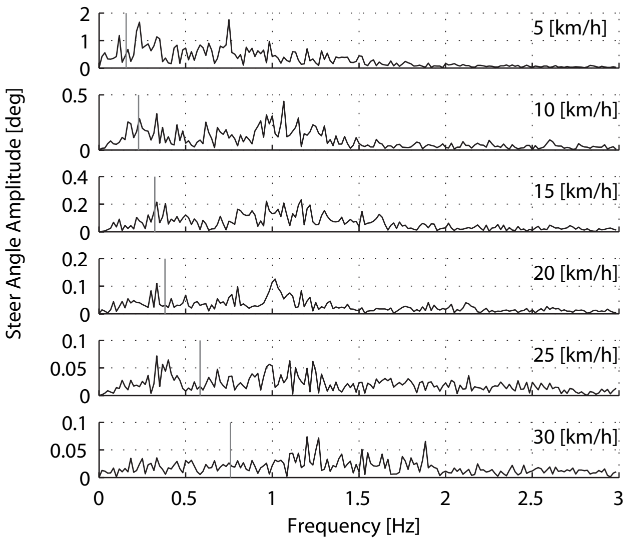


Figure 12. STEER ANGLE AMPLITUDE PLOT FOR THE SIX DIFFERENT SPEEDS FOR THE TOWING EXPERIMENT. VERTICAL LINE INDICATES THE BICYCLE & RIGID RIDER EIGENFREQUENCY.

angles were made at decreasing speeds. Figure 9 shows how the standard deviation of the steer angle reduces rapidly with increasing speed up to 20 km/h and from then on remains approximately constant. The figure also shows that the average steering amplitude at all speeds is lower than that for pedaling. The standard deviation is less than a degree for all speeds above 10km/h indicating that the average steer angle at the higher speeds is almost straight ahead!

The steer angle frequency spectrum for each of the speeds is shown in Fig. 12. It was expected that the rigid rider/bicycle weave frequency would be a dominant frequency in the frequency spectrum. However there appears to be no connection with the open loop weave frequency even in the unstable speed range. In fact the frequency spectrum shows a wide range of frequencies of similar amplitude at all the speeds and none of the speeds show a single dominant frequency. Therefore the assumption that the steering action whilst towing can be characterized by a single steering frequency, as it could for the normal bicycling experiment, does not hold for any of the speeds.

### Perturbing; Pedaling

The video footage showed that, as a result of the lateral perturbation, the bicycle was pulled laterally away from under the rider causing the bicycle to lean over and in turn cause a short transient lean motion of the rider's upper body. The upper body appears to only lag behind the lower body and bicycle during this destabilizing part of the perturbation maneuver. During the subsequent recovery of the bicycle to the upright, straight ahead position, no body lean could be noted other than that as a result of the normal pedaling.

A second phenomenon observable on the video footage, as shown in Fig. 13, is that at all speeds there is lateral knee motion during the short transient recovery process of the bicycle to the upright position. The lateral knee motion was very large during

Figure 13. SCREEN-SHOT DIRECTLY AFTER A PERTURBATION (LATERAL FORCE APPLIED FROM THE RIDER'S RIGHT BY A ROPE AT THE SADDLE TUBE) AT 5 KM/H. VERTICAL GREY LINE INDICATES THE BICYCLE MIDPLANE. NOTE THE LATERAL RIGHT KNEE MOTION AND STEERING ACTION AND THE SMALL UPPER BODY LEAN ACTION.

the 5 km/h measurement and much smaller at the higher speeds, but even at 30 km/h it is visible.

From the video footage it can be concluded that the angle that the handlebars are turned during and after a perturbation decreased with increasing speed as can also be seen in the measured steer angle data as shown in Fig. 9.

Figure 14 shows the frequency spectrum of the measured steer angle. Once again, for the higher speeds, the steer control action is carried out at the pedaling frequency. At the lower speeds (5 - 10 km/h) a wider frequency range is again present but the steering motion appears around the pedaling frequency. It is therefore again reasonable to assume that the steering motion is a function of a single frequency as for the normal bicycling experiment. Figure 11 shows the steering amplitude for the frequency with the maximum amplitude. Again the values for the highest speeds are similar to those of the standard deviation of the steer angle.

The frequency spectrum shows no significant steering motion taking place at the rigid rider/bicycle weave eigenfrequency for any of the speeds.

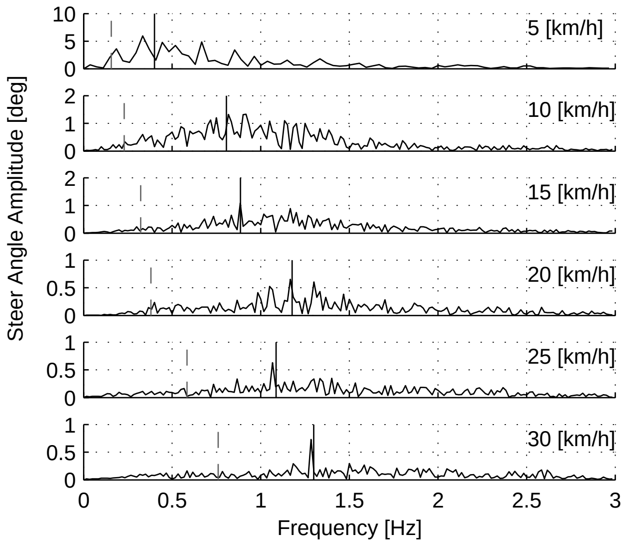


Figure 14. STEER ANGLE AMPLITUDE PLOT FOR THE SIX DIFFERENT SPEEDS FOR PERTURBATION EXPERIMENT. SOLID VERTICAL LINE INDICATES THE PEDALING FREQUENCY. DASHED VERTICAL GREY LINE INDICATES THE BICYCLE & RIGID RIDER EIGENFREQUENCY.

## CONCLUDING REMARKS

The observations show that human stabilizing control of the lateral motions of a bicycle during normal bicycling does not show any significant upper body lean, and that most of the stabilizing control actions are done with steering control. Only at very low forward speed is a second control added to the system: knee movement. Moreover, this lateral knee motion only occurs during pedaling. All steering actions are mainly performed at the pedaling frequency whilst the amplitude of the steering motion increases rapidly with decreasing forward speed.

## FUTURE WORK

Future work is directed at measuring the motion of a person riding a bicycle on a treadmill by means of a human motion capture system with active markers. This will allow for the identification of the motions of the individual body parts of the rider relative to bicycle and thus identify rider control in a quantitative manner.


## ACKNOWLEDGMENT

We would like to thank Knoek van Soest from the Faculty of Human Movement Sciences of the VU University Amsterdam for usage of their treadmill.


## REFERENCES


[1] Meijaard, J. P., Papadopoulos, J. M., Ruina, A., and Schwab, A. L., 2007. "Linearized dynamics equations for the balance and steer of a bicycle: a benchmark and review". *Proceedings of the Royal Society A,* **463**, p. 19551982.

[2] Kooijman, J. D. G., Schwab, A. L., and Meijaard, J. P., 2008. "Experimental validation of a model of an uncontrolled bicycle". *Multibody System Dynamics,* **19**, pp. 115–132.

[3] Kooijman, J. D. G., and Schwab, A. L., 2009. "Experimental validation of the lateral dynamics of a bicycle on a treadmill". In ASME 2009 International Design Engineering Technical Conferences & Computers and Information in Engineering Conference on Multibody Systems, Nonlinear Dynamics, and Control, IDETC/CIE 2009, August 30-September 2, 2009, San Diego, CA, USA.

[4] Cossalter, V., 2002. *Motorcycle Dynamics*. No. ISBN 0-9720514-0-6. Race Dynamics, Greendale, WI.

[5] Moore, J. K., Kooijman, J. D. G., Hubbard, M., and Schwab, A. L., 2009. "A method for estimating the physical properties of a combined bicycle and rider". In ASME 2009 International Design Engineering Technical Conferences & Computers and Information in Engineering Conference on Multibody Systems, Nonlinear Dynamics, and Control, IDETC/CIE 2009, August 30- September 2, 2009, San Diego, CA, USA.

[6] http://www.tam.cornell.edu/%7eals93/Bicycle/index.htm#Oct28.